

NbSe₃: Effect of uniaxial stress on the threshold field and fermiology

Jahyong Kuh, Y. T. Tseng, Keith Wagner, Jay Brooks, G. X. Tessema, and M. J. Skove
Department of Physics, Clemson University, Clemson, South Carolina 29634-1911

(Received 1 December 1997)

We have measured the effect of elastic strain ϵ on the threshold field E_T for the motion of the higher-temperature charge density wave (CDW) in NbSe₃. We find that E_T exhibits a critical behavior, $E_T \sim (1 - \epsilon/\epsilon_c)^\gamma$ where ϵ_c is about 2.6%, $\gamma \sim 1.2$. This expression remains valid over more than two decades of E_T , up to the highest fields of about 1.5 kV/m measured using pulse techniques. Neither γ nor ϵ_c is very sensitive to the impurity content of the sample. The transition temperature is linear with ϵ , and $dT_p/d\epsilon = 10$ K/% shows no anomaly near ϵ_c . The slope of the narrow band noise frequency versus the CDW current does not change appreciably with ϵ . Shubnikov-de Haas measurements show that the extremal area of the Fermi surface decreases with increasing ϵ . We conclude that there is a very intimate relationship between pinning and the fermiology in NbSe₃. [S0163-1829(98)12619-X]

I. INTRODUCTION

The recent discovery of the Aharonov-Bohm effect exhibited by the sliding charge density wave (CDW) in NbSe₃ has revived interest for the field of CDW.¹ Nonlinear conductivity is the outstanding characteristic of charge-density-wave materials.² The presence of a threshold field E_T , above which the resistance decreases, is the signature that the CDW can be made to move under a small electric field.^{3,4} The dependence of E_T on temperature (T), number of impurities (n_i),^{5,6} contact position, size,⁷ pressure,⁸ and uniaxial stress,^{9,10} has been extensively reported. Here we report further studies on the effect of elastic, uniaxial stress σ on E_T for the upper CDW in NbSe₃. This paper will show that $E_T \sim 1/|\sigma - \sigma_c|$, where $\sigma_c \approx 260$ GPa and that this is related to the change in fermiology as shown from low-temperature Shubnikov-de Haas (SdH) studies.

II. EXPERIMENTAL TECHNIQUES AND RESULTS

A. Samples

The experiments were conducted on nominally pure as well as Fe doped NbSe₃ samples. Fe doping was achieved by mixing either 4.7% or 7% of Fe in the starting materials; about one-tenth that much doping is expected in the resulting whiskers.¹¹ Samples of medium purity with a room temperature resistance ratio (RRR) of 70 were grown in house; the high purity samples, RRR > 200, were provided by R. E. Thorne. The samples were mounted on a stressing device described elsewhere.¹² Uniaxial stress was applied along the needle axis, the **b** crystal axis. The strain ϵ was directly measured, and can be converted to stress using the Young's modulus, $S_{22} \approx 100$ GPa.¹⁰ Four electrical contacts were made using conducting silver paint. Epoxy overlaid these contacts and formed the mechanical grips. Typical sample dimensions were $2000 \times 20 \times 1 \mu\text{m}^3$.

B. Effect of ϵ on the upper CDW

At low strain and low fields, the threshold field was determined using the conventional lock in or dV/dI technique. At high ϵ , where high electric fields are required to reach E_T , the pulse method was used. The duty cycle was less than

1%; with typical pulse width of 10 μs , and period 1 ms. The pulsed current and voltage were measured using a two channel boxcar signal averager, EG&G model 162. In this case, E_T was estimated from the plot of the chordal resistance R vs E or from the numerical derivative $\Delta V/\Delta I$. Previous studies^{9,10} have shown that uniaxial stress affects E_T indirectly by ϵ -induced changes in T_p and directly by enhancing the pinning strength. It was shown that the indirect effect can be disentangled by conducting the experiments at a constant reduced temperature $t = T/T_p(\epsilon)$ where $T_p(\epsilon)$ is defined at the peak in $dR(\epsilon)/dT$. Constant $t = 0.70$ was achieved by adjusting T for each value of ϵ . This value of t corresponds to the minimum value E_{\min} on the E_T versus t curve. It was previously shown that E_{\min} is proportional to the impurity concentration^{6,7} and assumed to correspond to bulk pinning rather than contact pinning. Although this paper is devoted to the study of the effect of ϵ on E_{\min} , for the sake of simplicity we will refer to it as the threshold field, or simply E_T .

Figure 1 shows a typical plot of E_T versus ϵ for an arbitrarily selected sample. E_T increases weakly at low strain and diverges near $\epsilon_c = 2.6 \pm 0.3\%$. The semilogarithmic plot of the same data shown in the inset indicates that E_T increases

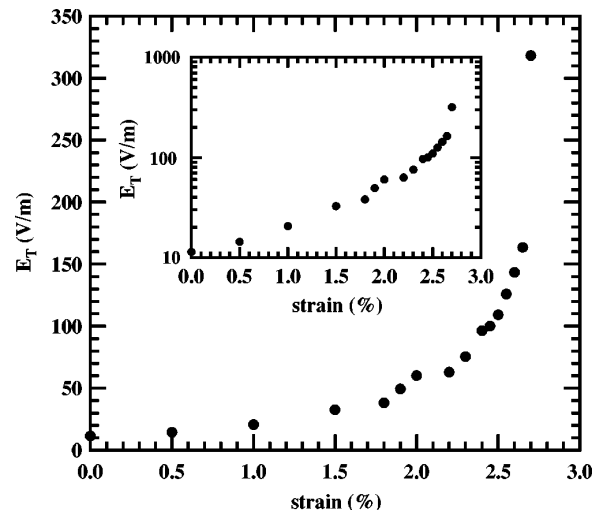


FIG. 1. E_T vs ϵ for a nominally pure sample. The inset shows a semilogarithmic plot of the same data.

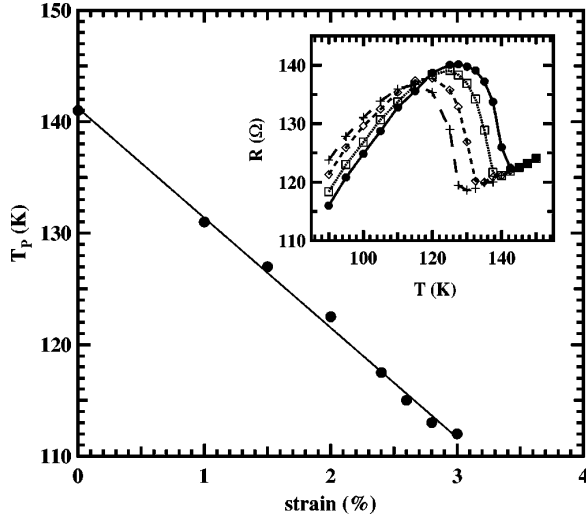


FIG. 2. The CDW transition temperature T_{p1} vs strain. T_{p1} decreases linearly with ε up to $\varepsilon=3\%$. Typical $R(\varepsilon)$ vs T plots are shown in the inset.

faster than a single exponential. In the few cases where we were able to pull beyond 2.6% strain, E_T exhibited a peak, decreasing above $2.6 \pm 0.3\%$. Figure 2 shows the strain dependence of T_p . T_p decreases linearly with increasing ε up to 3% at a rate $dT_p/d\varepsilon=10$ K/%. There is no apparent feature around $\varepsilon=2.6\%$, where E_T diverges. The inset in Fig. 2 shows a plot of R versus T for different values of ε . Note that the resistance anomaly $\Delta R(\varepsilon)=R_p(\varepsilon)-R_{fit}(\varepsilon)$ is independent of ε , where $R_p(\varepsilon)$ corresponds to the peak resistance for a given $R(\varepsilon)$ versus T plot, and $R(\varepsilon)_{fit}$ is the linearly extrapolated resistance at T peak from above 150 K. This result suggests that the CDW conductance ($G_{CDW} \sim n_{CDW}e\mu$, where e is the charge of the electron and μ the CDW mobility) at very large electric fields is independent of ε , which in turn implies that the fraction of condensed electrons n_{CDW} does not change appreciably with ε . This is consistent with narrow-band noise measurements, which showed almost no change in the slope of the CDW current versus the narrow-band frequency (dI_{CDW}/dF) with ε .¹³

C. Effect of ε on the Fermi surface

In this section we look for a connection between the effect of ε on the fermiology and the results reported in the previous section. The effect of ε on the dominant frequency of the Shubnikov–de Haas oscillations is reported. The magnetic field B_a was parallel to the (\mathbf{b},\mathbf{c}) plane and perpendicular to the smallest extremal area of the Fermi surface, with a typical frequency of 0.28 MG at $\varepsilon=0$.^{13–15} Two methods were used. The first method is the conventional method, B_a was increased slowly with the sample under constant strain. In the second method, B_a was constant while sweeping ε . The experiments were conducted at constant T between 3.0 and 4.2 K.

Figure 3(a) shows a typical plot of R vs H obtained using the conventional method, the inset shows $dR/d(1/H)$ versus $1/H$. The extremal area A was estimated from a plot of n versus $1/H$ for each value of ε . Figure 3(b) shows that A decreases nearly linearly with increasing ε . A detailed study of the effect of uniaxial stress on the Fermi surface will be reported elsewhere. In this paper we note that uniaxial stress

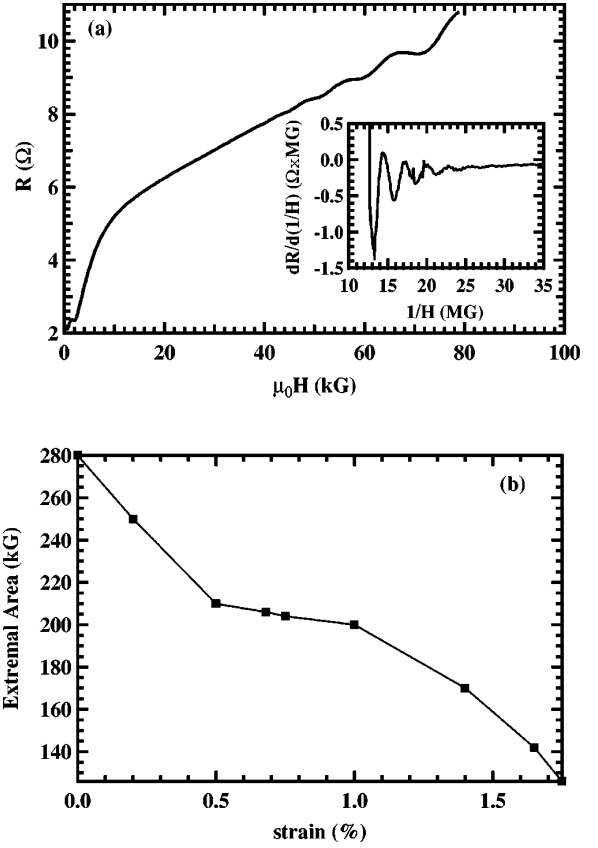


FIG. 3. (a) shows a typical plot of R vs H , which exhibits Shubnikov–de Haas oscillations. The derivative $dR/d(1/H)$ vs $1/H$ is shown in the inset. In (b) the extremal area, in units of kG, decreases smoothly with increasing ε .

suppresses A linearly at the rate of 0.09 MG/%, suggesting that the whole pocket would be wiped out for $\varepsilon \leq 3\%$. A study of the strain dependence of the conductance at low temperature shows that 90% of the conductance is wiped out for $\varepsilon \approx 2.6\%$. This suggests that this pocket plays a predominant role in the normal state conductance of NbSe₃ at low T .

The second method is equivalent to fixing the Landau tubes and shrinking the Fermi surface through them under the influence of ε . This leads to oscillations in the R vs ε plots as shown in Fig. 4(a). A systematic study of R versus ε for different values of B_a allows us to follow the strain and the field at which a given Landau tube is crossed. The results are summarized in Fig. 4(b), which shows a plot of ε vs B_a for each Landau tube identified by the integer next to its curve. The trajectory of a given Landau tube is nearly linear. This is consistent with the linear relationship between A and ε observed using the conventional technique. The solid lines in the figure are a guide to the eye. Note that at $B_a=0$ T, all the lines converge to nearly the same $\varepsilon_c^H \approx 2.6\%$. This suggests that this piece of the Fermi surface would be wiped out at about 2.6%. Below we will also show that ε_c^H is equal to the critical strain $\varepsilon_c^{E_T}$ derived from the critical plot of E_t of the upper CDW.

III. DISCUSSION

Possible pinning mechanisms of the CDW are bulk impurity pinning as discussed by Fukuyama-Lee-Rice¹⁶ (either

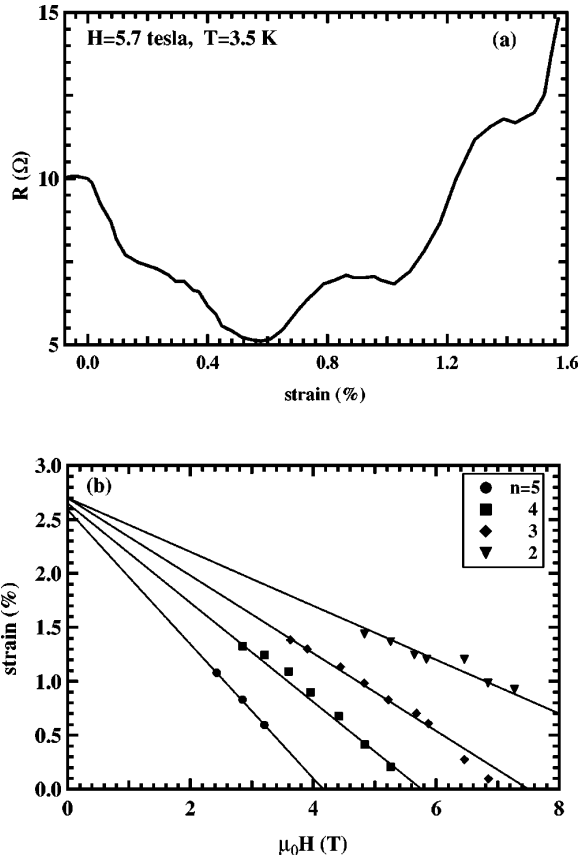


FIG. 4. (a) shows the oscillatory R vs ε plots for $B=5.4$ T. The oscillations are attributed to the intersection of the Landau tubes with the shrinking Fermi surface. (b) is a representation of this intersection in the (ε, B) space. The integers in the box correspond to the indices of the Landau levels.

strong or weak), commensurability pinning by the underlying lattice, or pinning by other defects such as surfaces, dislocations or contacts. The results in Fig. 3 could be due to one or a complex combination of the following effects: (1) strain-induced enhancement of the weak impurity pinning potential; (2) strain-induced crossover from weak pinning to strong pinning; (3) strain-induced incommensurate to commensurate transition; or (4) strain-induced enhancement of contact pinning. We now discuss each one of these effects separately, in inverse order of their likelihood.

Stress-induced enhancement of contact pinning is very unlikely. If this were the case, one would also expect a similar stress-induced enhancement of E_T for the lower CDW. However, previous studies have shown that stress does not enhance E_T for the lower CDW.^{9,10} In addition, Tseng, Tessema, and Skove have shown⁹ in the case of the upper CDW, E_T can be separated into two components, one attributed to contact pinning, and the other to bulk impurity pinning. They have argued that uniaxial stress does not enhance contact pinning. It also seems unlikely that uniaxial stress can affect surface pinning to that extent; if it did, our thinner samples would have shown a stronger effect.

The FLR model considers two possible kinds of impurity pinning: strong pinning and weak pinning. Several experiments indicate that pinning in NbSe_3 is due to weak pinning.^{6,7} Stress-induced crossover from weak pinning to strong pinning could be considered, in which case one would expect to see a change in the exponent γ with ε . γ is defined

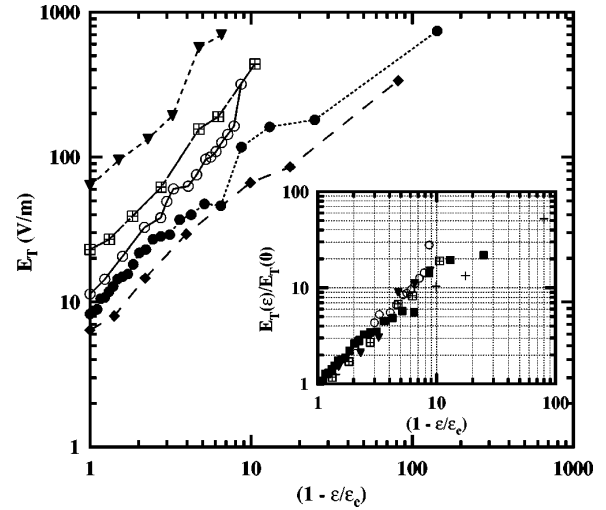


FIG. 5. A critical plot of E_T for five different samples. The full triangles and the crossed squares correspond to Fe-doped samples, 0.7% and 0.47%, respectively. The normalized threshold $e_T = E_T(\varepsilon)/E_T(0)$ is shown in the inset. Note that all five set of data fall on the same line.

in the next paragraph. The results show that γ is independent of ε and rule out this possibility as well. This is also supported by the fact that the same γ is obtained for the samples doped with Fe, which may be considered as a strong pinning impurity.

Experimental search for an incommensurate-commensurate transition (ICT) in CDW systems has not provided any clear evidence for these effects.¹⁷ A stress-induced ICT would lead to changes in $dT_P/d\sigma$ as well as solitonlike behavior near commensurability. Figure 2 shows that T_P does not show an anomaly near ε_c . Further, according to Fisher and Fisher¹⁸ the approach to commensurability should behave critically with an exponent of $\frac{1}{2}$ (for 2D) or be logarithmic. Figure 5 shows such a critical plot of E_T versus $(1 - \varepsilon/\varepsilon_c)$ in a log-log scale. A plot for the normalized threshold field

$$e_T = E_T/E_{T_0} = (1 - \varepsilon/\varepsilon_c)^\gamma, \quad (1)$$

where E_{T_0} is the threshold field at zero strain and ε_c and γ are adjustable parameters, is shown in the inset. In the following we will replace ε_c with $\varepsilon_c^{E_T}$ in order to differentiate it with the critical strain defined from the fermiology study. Note that the results for five different samples with different impurity content, and Fe impurity fall along the same line, with nearly the same parameters. A list of the values of $\varepsilon_c^{E_T}$ for different samples is shown in Table I. Although the figure is in qualitative agreement with Fisher and Fisher's prediction that E_T should behave critically in an ICT, the exponents are not in quantitative agreement with the model. Our larger samples are most likely 3D, and the exponent is not $1/2$; therefore the critical behavior cannot be explained by a simple approach to commensurability. On the other hand, an argument in favor of ICT can be made based on the divergence of E_T . Since commensurability pinning is much stronger than impurity pinning, E_T is much more sensitive to stress-induced ICT than T_P is. This issue could be resolved using structural studies as a function of strain.

TABLE I. The fitting parameters $\varepsilon_c^{E_T}$ and γ are shown together with other relevant parameters such as the nominal purity, the RRR, and the threshold field E_T . Only the nominal Fe doping levels are given.

Sample	RRR	$\varepsilon_c^{E_T}\%$	γ	E_T (V/m)
Pure	250	2.6	1.58	8.0
Pure	200	3	1.23	11
Pure		2.6	1.23	6.3
Pure		2.6	1.66	10
4.7% Fe		3.2	1.14	28
4.7% Fe		2.6	1.08	31
7% Fe		2.7	1.23	63

According to the FLR theory,¹⁶ the threshold field for weak pinning is given by

$$eE_T\lambda \propto \frac{\Delta^2}{E_F} (\xi_x, \xi_y, \xi_z n_i^2) V_0^{[4/(4-D)]}, \quad (2)$$

where λ is the wavelength of the CDW, ξ_x , ξ_y , and ξ_z are coherence lengths for the CDW amplitude, E_T the threshold field, e the electric charge, E_F the Fermi energy, V_0 the impurity potential, and D the dimensionality.¹⁶ Stress could affect any or all of the parameters in Eq. (2). However, for the sake of simplicity we will discuss separately the terms that are susceptible to change with T_P . In the conventional BCS model the CDW gap is proportional to T_P , $\Delta/T_P=4.8$ for NbSe₃.¹ As in previous pressure work,⁸ uniaxial stress-induced enhancement of the electron-phonon coupling constant could be considered. However, it would take more than an order of magnitude of change in order to account for our results. On the other hand if, in a first approximation, one assumes that this ratio is not affected by ε , Δ would decrease with T_P , which would lead to a decrease in E_T , contrary to our results. Another possibility is a strain-induced decrease in E_F . But the normal state conductivity around T_P is a weak function of ε , even up to 3%, suggesting that E_F is not strongly affected by ε . One likely possibility is that V_0 is strongly affected by stress. Suppose there is a stress-induced tuning of the matching between the phase and wavelength of the CDW and the Friedel oscillations.¹⁹ Then, although the changes in E_F due to the vanishing of this small pocket could be negligible, it could be sufficient to lead to a rapid increase

of V_0 . This mechanism would be independent of the type of impurity and concentration, in agreement with our experiments. One other possibility is that the pocket screens the impurity, and V_0 increases when the pocket disappears. Below we will discuss the difference between the upper and lower CDW.

In a study of the combined effect of magnetic field and strain, Parilla, Carey, and Zettl²⁰ have shown that uniaxial stress and $\mu_0 H$ act on the same piece of the Fermi surface. This was confirmed by Tseng, Tessema, and Skove²¹ who observed pronounced effect of strain on the resistance and thermopower of NbSe₃ below 59 K. Shi, Chepin, and Ross²² have conducted NMR experiments to study the density of states on the different chains in NbSe₃. Although magnetic fields effects on the Ohmic regime, below E_T , are much more pronounced below the second transition than below T_{p1} , their results show that most of the changes in FS are due to changes in density of states on the chain associated with the upper CDW rather than the lower CDW. This supports the notion that the strain-induced changes in E_T of the upper CDW are associated with changes in the Fermi surface most closely associated with the chain corresponding to the upper CDW. The relatively small effects on the density of states associated with the lower CDW could account for the rather weak effect on the E_T of the lower CDW.

IV. CONCLUSION

It was previously reported that uniaxial stress enhances E_T for the upper CDW in NbSe₃. In this paper we report a systematic study of the effect of ε on E_T , T_P , and the Fermi surface of this compound. We show that the divergence of E_T near 2.6% strain is intimately related to stress-induced changes in fermiology. We propose that the two most likely possibilities for this phenomena are (1) a stress induced incommensurate to commensurate transition (2) or more likely an ε driven matching of the Friedel oscillations and the CDW oscillations of the upper CDW. Structural studies under stress should give a further insight into the subject.

ACKNOWLEDGMENTS

The authors would like to thank Professor John C. McCarten for his valuable comments and suggestions, and R. E. Thorne for his high purity samples. This work was supported by the National Science Foundation under Grant No. DMR 9312530.

¹Y. I. Latyshev *et al.*, Phys. Rev. Lett. **78**, 919 (1997).

²For comprehensive review of CDWs see *Electronic Properties of Quasi-One-Dimensional Materials*, edited by P. Monceau (Reidel, Dordrecht, 1985); C. Schlenker *et al.*, in *Low-Dimensional Electronic Properties of Molybdenum Bronzes and Oxides* (Kluwer Academic Publishers, Dordrecht, 1989); and *Charge Density Waves in Solids*, edited by L. P. Gorkov and G. Gruner (Elsevier, Amsterdam, 1989).

³P. Monceau *et al.*, Phys. Rev. Lett. **37**, 602 (1976).

⁴N. P. Ong and P. Monceau, Phys. Rev. B **16**, 3443 (1977).

⁵N. P. Ong *et al.*, Phys. Rev. Lett. **42**, 811 (1979); J. W. Brill *et al.*, Phys. Rev. B **23**, 1517 (1981).

⁶D. A. DiCarlo *et al.*, Phys. Rev. B **42**, 7643 (1990).

⁷J. C. McCarten *et al.*, Phys. Rev. Lett. **63**, 2841 (1989); D. V. Borodine *et al.*, Physica B **143**, 73 (1986); J. Yetman and J. C. Gill, Solid State Commun. **62**, 201 (1987).

⁸G. Mihaly and P. Canfield, Phys. Rev. Lett. **64**, 459 (1990).

⁹Y. T. Tseng *et al.*, Phys. Rev. B **48**, 4871 (1993).

¹⁰R. S. Lear *et al.*, Phys. Rev. B **29**, 5656 (1984).

¹¹Y. Gong *et al.*, Phys. Rev. B **51**, 12 975 (1995).

¹²D. R. Overcash *et al.*, Phys. Rev. B **1**, 214 (1971).

¹³J. Brooks, Msc. thesis, Clemson, 1992.

¹⁴P. Monceau and A. Briggs, J. Phys. C **11**, L465 (1978).

¹⁵R. M. Fleming *et al.*, Phys. Rev. B **17**, 1634 (1978).

¹⁶H. Fukuyama and P. A. Lee, Phys. Rev. B **17**, 535 (1978); P. A. Lee and T. M. Rice, *ibid.* **19**, 3970 (1979).

¹⁷George Gruner, *Charge Density Waves in Solids* (Addison-Wesley, Reading, MA, 1994).

¹⁸M. E. Fisher and D. S. Fisher, Phys. Rev. B **25**, 3192 (1982).

¹⁹I. Tuto and A. Zawadowski, Phys. Rev. B **32**, 2449 (1985).

²⁰P. Parilla *et al.*, Solid State Commun. **64**, 417 (1987).

²¹Y. T. Tseng *et al.*, Solid State Commun. **82**, 841 (1992).

²²J. Shi *et al.*, Phys. Rev. Lett. **69**, 2106 (1992).